Am J Transl Res 2015;7(6):1009-1020
www.ajtr.org /ISSN:1943-8141/AJTR0009160

Original Article

Phosphorylation of EZH2 at T416 by CDK2 contributes to the malignancy of triple negative breast cancers

Cheng-Chieh Yang[1,2*], Adam LaBaff[1,2*], Yongkun Wei[1*], Lei Nie[1*], Weiya Xia[1], Longfei Huo[1], Hirohito Yamaguchi[1], Yi-Hsin Hsu[1], Jennifer L Hsu[1,3,4], Dongping Liu[1], Jingyu Lang[1], Yi Du[1], Huang-Chun Lien[5], Long-Yuan Li[3,4], Rong Deng[1], Li-Chuan Chan[1,2], Jun Yao[1], Celina G Kleer[7], Gabriel N Hortobagyi[6], Mien-Chie Hung[1,2,3,4]

[1]Department of Molecular and Cellular Oncology, The University of Texas MD Anderson Cancer Center, Houston, Texas 77030; [2]Graduate School of Biomedical Sciences, The University of Texas Health Science Center at Houston, Houston, Texas 77030; [3]Center for Molecular Medicine, and Graduate Institute of Cancer Biology, China Medical University, Taichung 404, Taiwan; [4]Department of Biotechnology, Asia University, Taichung 413, Taiwan; [5]Department of Pathology, College of Medicine, National Taiwan University, Taipei 106, Taiwan; [6]Department of Breast Medical Oncology, The University of Texas MD Anderson Cancer Center, Houston, Texas 77030; [7]Department of Pathology, University of Michigan Medical School, Ann Arbor, Michigan 48109. [*]Equal contributors.

Received April 15, 2015; Accepted June 3, 2015; Epub June 15, 2015; Published June 30, 2015

Abstract: Triple-negative breast cancer (TNBC), which is closely related to basal-like breast cancer, is a highly aggressive subtype of breast cancer that initially responds to chemotherapy but eventually develops resistance. This presents a major clinical challenge as there are currently no effective targeted therapies available due to its lack of HER2 and estrogen receptor expression. Here, we show that cyclin E and the enhancer of zeste 2 (EZH2) are closely co-expressed in TNBC patients, and cyclin E/CDK2 phosphorylates EZH2 at T416 (pT416-EZH2) *in vivo*. Phosphorylation of EZH2 at T416 enhances the ability of EZH2 to promote TNBC cell migration/invasion, tumorsphere formation, and *in vivo* tumor growth. In addition, high pT416-EZH2 correlates with poorer survival in TNBC patients. These findings suggest that pT416 has the potential to serve as a therapeutic biomarker for the aggressive forms of breast cancer and provide a rationale for the use of CDK2 inhibitors to treat TNBC.

Keywords: CDK2, EZH2, phosphorylation

Introduction

Breast cancer is a heterogeneous disease that can be classified into five intrinsic subtypes, including luminal A, luminal B, HER2-enriched, normal breast-like, and basal-like breast cancer (BLBC), based on the gene expression profiling [1, 2]. In contrast, breast cancer that lacks the expression of HER2, progesterone receptor (PgR), and estrogen receptor (ER) is also defined as triple-negative breast cancer (TNBC) [3, 4]. TNBC is also heterogeneous and further classified into six subtypes according to gene expression profiles [5]. It has been shown that BLBC is closely related to TNBC and around 80% of BLBC is triple negative [4, 6-8]. BLBC and TNBCs indeed share common features, such as high proliferative rates and enhanced cell invasion capabilities with undifferentiated carcinomas [4, 9]. Clinically, both BLBC and TNBC are considered as the most aggressive and deadly subtype of breast cancer, displaying high rates of drug resistance, metastasis, and post-surgical re-occurrence [10-12]. Since hormone and HER2-targeted therapies are not effective against TNBC, chemotherapy is the primary systemic treatment for TNBC patients. Although pathologic complete response rates to chemotherapy in TNBC patients is actually higher than non-TNBC patients, TNBC patients who have residual disease after chemotherapy will eventually have worse outcome than non-TNBC patients [13]. Therefore, further in-depth understanding of the BLBC/TNBC biology is required for the betterment of patient therapy.

The enhancer of zeste 2 (EZH2), the histone methyltransferase subunit of polycomb repres-

sive complex 2, initiates transcriptional repression through histone 3 lysine 27 tri-methylation (H3K27me3) of its target gene promoter regions [14, 15]. Expression of EZH2 in TNBC patients has been reported to correlate with advanced tumor stage and increased mortality [16, 17]. EZH2 also enhances tumor progression, metastasis, angiogenesis, and the population of breast tumor initiating cells (BTIC) [18, 19]. Independently, cyclin E expression has also been reported to correlate with poor prognosis and increased mortality in TNBC patients [20]. Furthermore, cyclin-dependent kinases, CDK1 and CDK2 can phosphorylate EZH2 at various sites within EZH2 and regulate its activity [21-25]. For example, phosphorylation of EZH2 at T345 by CDK1 was shown to upregulate its binding to HOTAIR ncRNA [21], and phosphorylation at T345 and T487 by CDK1 and CDK2 was shown to regulate epigenetic gene silencing [22, 23]. In addition, T416 was shown to be phosphorylated by cyclin A/CDK2 or cyclin B/CDK1 *in vitro* [21, 25]. Interestingly, phosphorylation of EZH2 at T416 serves as a binding site for NIPP1, which inhibits PP1-mediated dephosphorylation of EZH2 and regulates EZH2 function [25]. Here, we investigated the role of EZH2 T416 phosphorylation in TNBC cells and assessed its relationship to survival of TNBC patients.

Materials and methods

Reagents and plasmids

SNS032 and CDK2 inhibitor II were purchased from Calbiochem. Roscovitine was purchased from LC Labs. Generation of $EZH2^{T416A}$ and $EZH2^{T416D}$ point mutants was performed using Quick Change site-directed mutagenesis kit from Stratagene. The Cylin E, $CDK2^{WT}$, and $CDK2^{DN}$ expression plasmids were purchased from Addgene. All lentiviral pLKO.1 expression and shRNA encoding plasmids were provided by Academica Sinica (Taipei, Taiwan).

In vitro kinase and ^{35}S-methionine labeling GST pull-down assays

Purified GST-EZH2 fragments were incubated with active cyclin E-CDK2 complex (New England Biolabs) in the presence of 50 mM ATP in kinase buffer containing 5 μCi ^{32}P-ATP for 30 min at 30°C. The reaction products were resolved via SDS-PAGE and ^{32}P-labeled products were detected using autoradiography. The *in vitro* ^{35}S-methionine labeling was performed using *in vitro* translation assay kit from Promega. For GST pull-down assays, the GST-EZH2 fragments were each incubated at 4°C overnight with 5 μl of *in vitro* translated HA-$CDK2^{WT}$. The GST-tagged proteins were recovered by incubating the reaction at 4°C for 3 h with 20 μl glutathionine-Sepharose beads (Roche). The pelleted beads were washed three times with 1 ml buffer (20 mM Tris-HCl at pH 7.5, 150 mM NaCl, 10% glycerol, 15 Triton X-100 and 2 mM EDTA. Heat denatured samples were resolved via SDS-PAGE. ^{35}S-methionine labeled products were detected using autoradiography.

Cell culture

All cell lines used were purchased from ATCC, and their validation was performed in the Characterized Cell Line Core Facility, MD Anderson Cancer Center. Cell lines used include 293T, a human embryonic kidney cell line; T47D, a human mammary ductal carcinoma cell line from pleural effusion; MDA-MB-231 a human mammary adenocarcinoma cell line from pleural effusion. Unless designated otherwise, all cells were cultivated in Dulbecco's Modified Eagle's Medium/F12 supplement (DMEM/F12) supplemented with 10% heat-inactivated fetal bovine serum (FBS), Penicillin/Streptomycin (100 U, 100 μg/ml) at 37°C in a humidified atmosphere with 5% CO_2. Neomycin- and puromycin-resistant stable cell lines were maintained in G418 (500 μg/ml) and puromycin (2.5 μg/ml), respectively.

Cell growth, colony formation, soft-agar, and cell migration and invasion assays

Cell growth was determined by calcein AM assay kit according to the manufacturer's protocol (Cell Biolabs). Cell growth was also determined by MTT assay. Cells (3×10^3) per well were seeded in 96-well plates. After adherence, 20 μM MTT was added and incubated for 24 h before addition of lysis buffer (20% SDS and 50% DMSO). After incubation, absorbance was measured at 570 nm. For 2D colony formation assay, the cells were seeded at ranges of 500, 1000, and 5000 cells per well in a 6-well dish and grown for 10 days in 10% FBS-containing medium. Colonies were fixed and stained with crystal violet for 5 min, followed by

washing with PBS. Colonies were counted under microscope for quantitation. For the soft agar transformation assay, 5×10^4 cells were seeded in 1.5 ml DMEM with 10% FBS and 0.3% agarose and overlaid onto 3 ml DMEM with 10% FBS and 0.6% agarose in each well of a 6-well plate. After 2 to 3 weeks, colonies larger than 200 μm in diameter were counted. Migration was measured in 24-well Boyden chamber plates with an 8 μm pore size polycarbonate filter (BD Biosciences). The lower chamber contained 0.75 ml of 10% FBS medium. The upper chamber contained 1×10^4 cells seeded in serum-free medium and incubated at 37°C for 24 h. The chamber filters were fixed with 4% glutaraldehyde in PBS and stained with crystal violet. Remaining cells were removed from on top of the filter with a cotton swab. The migrated cells were then counted under microscope for quantitation after destaining. Invasion potential of the cancer cells was performed in 24-well Boyden chamber plates with an 8 μm pore size polycarbonate filter coated with growth factor free Matrigel (BD Biosciences). The lower chamber contained 0.75 ml of 10% FBS medium. The upper chamber contained 5×10^4 to 1×10^5 cells seeded in serum-free medium. The invasive cells were fixed and stained as describe above.

Drug treatment

CDK2 inhibitor treatment was administered to cells at IC_{50} concentrations for SNS032, CDK2 inhibitor II, and Roscovitine. The inhibitor was replaced daily. Cell growth and cell viability were determined as above described.

Immunohistochemistry, immunoblotting, and immunoprecipitation

Immunohistochemical staining, immunoblotting, and immunoprecipitation were performed as previously described with the following antibodies: EZH2, cyclin E, CDK2, NPM, p-NPM (Cell Signaling), tubulin, and actin (Sigma). Anti-pT416-EZH2 monoclonal antibody was raised by immunization of mouse with phospho-peptides (ANSRCQ-pT416-PIKMKPNIE).

Side-population determination and tumorsphere formation assay

Breast cancer cells were grown to confluence of 80-90% in a 2D monolayer in 10% FBS medium. Cells were then trypsinized, washed 3 times in PBS, and the single cells were incubated in 5 μg/ml of Hoechest 33342 in 5% FBS-containing medium at 37°C for 2 h. Control cells were treated with 1 μM of P-glycoprotein inhibitor Tariguidar (Selleckchem) plus Hoechest 33342. The side population gating was set based on Tariguidar-treated cells. Tumorsphere formation assays were performed in low adhesive plate with complete Mammocult medium (Stem Cell Technology). The single cells were seeded at density of 1×10^4 to 10^5 cells per well. Sphere formation was then assessed at day 7 or day 10. Inhibitor was added after collecting and adjusting tumorsphere to 200 spheres per well in a 12-well plate. The pre-formed tumorspheres were collected with cell strainer (80 μm; BD Biosciences), and these pre-formed tumorspheres at the same density were treated with vehicle or CDK2 or EZH2 inhibitor at 2 μM and 5 μM, respectively, for 7 days. The medium containing inhibitors was renewed every other day.

Animal studies

Tumorigenesis assays were performed in an orthotopic breast cancer mouse model. MDA-MB-231 cells (4×10^6) with lentiviral-stable expression of $EZH2^{WT}$, $EZH2^{T416A}$, or $EZH2^{T416D}$ were injected into mammary fat pads of female nude mice (5 per group). Tumor size was measured every 3 days with a caliper, and tumor volume was determined using the formula: $L \times W^2 \times 0.52$, where L is the longest diameter and W is the shortest diameter.

Statistical analysis

SPSS software (version 21) was used for statistical analysis (IBM). An univariate analysis was used to determine the variable distributions. Categorical variables among the groups were compared with the x-squared test or Fisher's exact test if 20% of the expected values were smaller than five. Continuous variables were analyzed using the Student's t-test. A p value of < 0.05 was considered statistically significant.

Results

Cyclin E/CDK2 associates with and phosphorylates EZH2 in TNBC

Because both EZH2 and cylin E expression correlate with poor prognosis and increased mor-

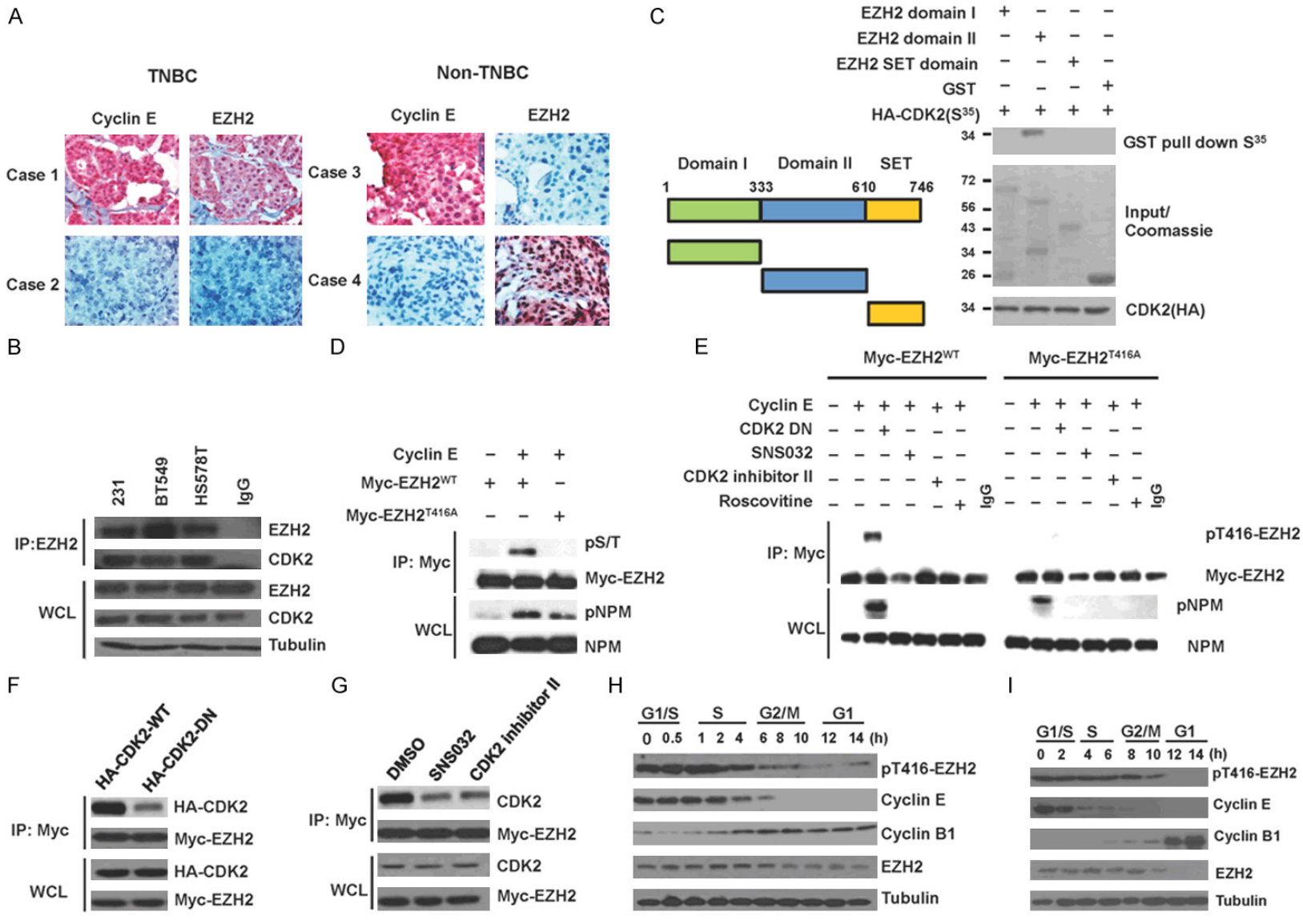

Figure 1. Cyclin E/CDK2 interacts with and phosphorylates EZH2 at T416. A. Cohort of 122 primary triple-negative breast cancer tissues and 125 of non-triple negative patients on tissue microarrays were subjected to IHC staining with cyclin E and EZH2 antibodies. Representative images are shown. B. Lysates from three different TNBC cell lines were subjected to immunoprecipitation (IP) using anti-EZH2 antibody, followed by Western blot using anti-EZH2 and anti-CDK2 antibodies.

C. GST pull-down assay was performed with GST-EZH2 fragments and *in vitro* translated HA-CDK2. The fragments used in this assay are shown on left. D. 293T cells were transfected with the indicated plasmids, and myc-tagged EZH2 was immunoprecipitated with anti-myc antibody. EZH2 phosphorylation was then determined by Western blot with anti-phospho-serin/threonine (pS/T) antibody. Nucleophosmin (NPM) and phosphorylated NPM (p-NPM), which is a direct substrate of cyclin E/CDK2, were used as control. E. 293T cells were transfected with the indicated expression plasmids and treated with SNS032 (a CDK2 inhibitor), CDK2 inhibitor II, and Roscovitine (a CDK1/2 inhibitor). Then, the cell lysates were subjected to IP using anti-myc antibody, followed by Western blot with anti-myc, anti-p-NPM, anti-NPM, or anti-phospho-T416 EZH2 antibodies. F. 293T cells were expressed with HA-tagged wild-type CDK2 (HA-CDK2) or dominant negative CDK2 (HA-CDK2-DN) together with myc-EZH2 and then subjected to IP/Western blot analysis using the indicated antibodies. G. 293T cells were expressed with CDK2 and myc-EZH2 and treated with the indicated CKD2 inhibitors. The cell lysates were then subjected to IP/Western blot analysis with the indicated antibodies. H. HeLa cells were synchronized and released using double-thymidine block and monitored from 0, 0.5 to 14 h after removal of thymidine block. I. MDA-MB-231 cells were synchronized and released using double-thymidine block and monitored from 0, 2, to 14 h after removal of thymidine block.

Table 1. Relationship between EZH2 and Cyclin E expression in TNBC patients

		EZH2 Expression			
		Negative	Positive	Total	*p* value
Cyclin E	Negative	37 (30.3%)	13 (10.7%)	50 (41%)	
	Positive	30 (24.6%)	42 (34.4%)	72 (59%)	
Total		67 (54.9%)	55 (45.1%)	122 (100%)	P < 0.0001

Table 2. Relationship between EZH2 and Cyclin E expression in non-TNBC patients

		EZH2 Expression			
		Negative	Positive	Total	*p* value
Cyclin E	Negative	46 (36.8%)	64 (51.2%)	110 (88%)	
	Positive	5 (4%)	10 (8%)	15 (12%)	
Total		51 (40.8%)	74 (59.2%)	125 (100%)	P = 0.53

tality in TNBC [17, 20], we first asked whether there is a functional relationship between cyclin E/CDK2 and EZH2 in TNBC. A cohort of 122 primary TNBC and of 125 non-TNBC tissues [26] were subjected to immunohistochemical (IHC) staining for cyclin E and EZH2 with specific antibodies, and the results indicated that high cyclin E and high EZH2 expression level are closely correlated in TNBC (P < 0.0001) (**Figure 1A** and **Table 1**), but not in the non-TNBC cohort (P = 0.53; **Figure 1A** and **Table 2**). These results suggest a possible functional link between cyclin E/CDK2 and EZH2 in TNBC. Previously, one study showed that CDK2, the major enzymatic partner of cyclin E [27], physically associates with EZH2 in prostate cancer cells [22]. To investigate their relationship in TNBC, we validated this interaction in several TNBC breast cancer cell lines, includeing MDA-MB-231, BT549, and Hs578t cells, by co-immunoprecipitation assays (**Figure 1B**). We also mapped the CDK2-interacting domain in EZH2 by GST pull-down assay. *In vitro* translated S^{35}-labeled HA-CDK2 was co-incubated with a N-terminal GST-tagged EZH2 fragment containing either EZH2 function domain I (amino acid residues 1-333), domain II (amino acid residues 334-610), or domain III, (amino acid residues 611-746; also known as the SET domain). The results revealed that CDK2 associated predominantly with domain II of EZH2 (**Figure 1C**). It has previously shown that EZH2 can be phosphorylated by cyclinA/CDK2 complex at T416 *in vitro* [25]. To further validate if cyclin E/CDK2 complex can also phosphorylate the same site, we performed an *in vitro* protein kinase assay using cyclin E/CDK2 complex and different GST-EZH2 fragments. The results showed that domain II was phosphorylated by cyclin E/CDK2, and the phosphorylation was virtually diminished by alanine substitution at T416 (T416A; Supplementary Figure 1, right). Also, *in silico* analysis (Supplementary Figure 1, left) revealed that T416 in domain II is indeed an evolutionary conserved CDK2 phosphorylation motif [28]. Next, we further verified T416 phosphorylation in EZH2 by cyclin E/CDK2 *in vivo*. We ectopically expressed myc-tagged full-length wild-type EZH2 ($EZH2^{WT}$) or T416A mutant EZH2 ($EZH2^{T416A}$) together with cyclin E expression plasmid in 293T cells. Myc-$EZH2^{WT}$ and Myc-$EZH2^{T416A}$ were then immunoprecipitated by anti-myc antibody, followed by Western blot analysis with anti-phospho-serine/threonine antibody. As shown in **Figure 1D**, we observed

EZH2 phosphorylation in $EZH2^{WT}$ but not in $EZH2^{T416A}$. In contrast to CDK1 whose major phosphorylation site of EZH2 is T487 [23], our current results suggest that T416 may be a major phosphorylation site of CDK2 *in vivo*.

To further validate cyclin E/CDK2 complex-mediated phosphorylation at T416 *in vivo*, we generated a mouse monoclonal antibody against the pT416-containing peptide, which was characterized by a peptide dot blot assay to determine its specificity and sensitivity (Supplementary Figure 2). Then, we used anti-pT416 EZH2 antibody to evaluate EZH2 phosphorylation *in vivo*. We ectopically expressed $EZH2^{WT}$ or $EZH2^{T416A}$ with control vector, cyclin E alone, or cyclin E plus dominant-negative mutant CDK2 (DN-CDK2) in 293T cells, and then treated some of them with various CDK2 inhibitors (SNS032, CDK2 inhibitor II, and Roscovitine; **Figure 1E**). Cyclin E strongly enhanced T416 phosphorylation in $EZH2^{WT}$ but not in $EZH2^{T416A}$ mutant (**Figure 1E**). On the contrary, pT416-EZH2 was not detectable in cells expressing DN-CDK2 or in cells treated with different CDK2-specific inhibitors (**Figure 1E**). In addition, wild-type CDK2 associated with EZH2 more strongly than DN-CDK2, which was attenuated by the addition of CDK2 inhibitors (**Figure 1F** and **1G**). Taken together, these results demonstrate that cyclin E/CDK2 is the kinase complex that phosphorylates EZH2 at T416 *in vivo*.

EZH2 is a cell cycle-regulated protein transcriptionally controlled by the Rb/E2F pathway at the beginning of G1/S phase of the cell cycle [29]. CDKs are well known for their role in regulating cell cycle checkpoints. To study the cell cycle dependency of the EZH2 phosphorylation at T416, we established a cell culture system of synchronized cell populations to monitor pT416 with specific anti-pT416 EZH2 antibodies. HeLa cells, a canonical cell line model for cell cycle synchronization, were used in addition to MDA-MB-231 TNBC cells. Cells were synchronized at the G1/S phase of cell cycle by double thymidine-block and then released by removal of thymidine. The level of EZH2 pT416 was highest during G1/S that also corresponded to a peak in cyclin E expression in both HeLa (**Figure 1H**) and MDA-MB-231 (**Figure 1I**) cells. Both pT416 and cyclin E expression decreased as cells progressed toward G2/M. Notably, total EZH2 protein level was also decreased in G1/S (**Figure 1H** and **1I**). These results suggest that T416 phosphorylation of EZH2 is cell cycle-dependent, and tightly controlled by its upstream regulator cyclin E/CDK2.

CDK2-dependent phosphorylation of EZH2 confers more malignant phenotypes in breast cancer cells

Since increased cyclin E level closely correlated with elevated EZH2 expression in the TNBCs (**Figure 1A** and **Tables 1** and **2**), and TNBCs are of higher proliferative rate and invasive potential [5], we asked whether cyclin E/CDK2-EZH2 pathway plays a role in their high proliferative rate and enhanced migration and invasive potential of TNBC. To evaluate the effect of pT416-EZH2 on proliferation rate and anchorage-independent growth of breast cancer cells, we first established stable MDA-MB-231 cells expressing $EZH2^{WT}$ or two different T416 mutants, phospho-deficient $EZH2^{T416A}$ or phospho-mimic $EZH2^{T416D}$ (**Figure 2A**). Under two-dimensional (2D) cell culturing conditions, overexpression of neither WT nor mutant EZH2 significantly affected the proliferation rate of MDA-MB 231 as measured by MTT (**Figure 2B**) or colony formation (**Figure 2C**) assays. However, when under 3D growth conditions (soft-agar anchorage independent assay), $EZH2^{T416A}$ mutant-expressing cells exhibited reduction of colony-formation ability compared to those expressing $EZH2^{WT}$ (**Figure 2D**). Conversely, expression of $EZH2^{T416D}$ increased the colony-formation ability of MDA-MB-231 cells compared to $EZH2^{WT}$ expressing cells (**Figure 2D**). The increased colony-forming ability of T416D mutant was also accompanied by enhanced migration (**Figure 2E**) and invasion (**Figure 2F**). Together, these results suggest that EZH2 T416 phosphorylation plays an important role in governing anchorage-independent transforming, migration, and invasive activities of TNBC cells.

Phosphorylation of EZH2 at T416 by CDK2 is required for expansion and maintenace of breast tumor-initiating cells

EZH2 promotes the expansion of very early lineage progenitors in a variety of tissues and cancer stem cells, including breast cancer stem cells (also referred to as breast tumor initiating cells or BTICs) [18, 19]. However, the mechanisms regulating EZH2 function in maintaining the BTICs are not yet clear. Knowing that EZH2

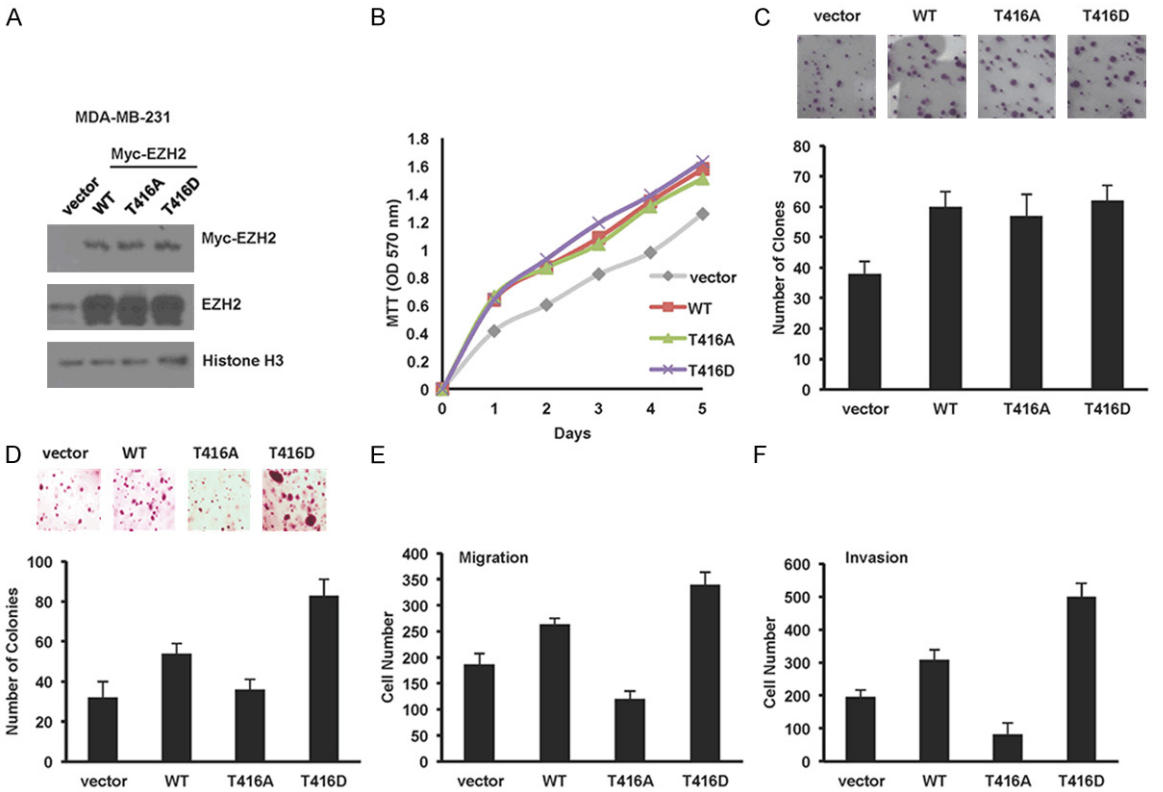

Figure 2. Phosphorylation of EZH2 T416 enhances migration and invasion potential and anchorage-independent growth. (A) Stable cell lines of MDA-MB231 were established by lentiviral infection. EZH2^{WT}, EZH2^{T416A} and EZH2^{T416D} protein levels in the stable cell lines were determined by Western blot analysis with the indicated antibodies. (B) Cell proliferation rates of the stable cell lines shown in (A) were determined with MTT assay. (C and D) Colony formation abilities of the stable cell lines described above were determined in 2D dilution assay (C) and 3D soft-agar assay (D). The number of colonies in one area was counted and is shown as bar graphs. Representative images are shown above. (E and F) Migration and invasive potential of the stable cell lines shown in (A) were performed in Boyden chamber without (E) or with (F) coated Matrigel. Error bars, ± SD.

T416 phosphorylation was able to enhance colony formation in 3D culture condition, which is one of the characteristics of BTICs (**Figure 2D**), we first determined the effect of CDK2 and EZH2 on BTICs. We knocked down CDK2 or EZH2 in MDA-MB231 cells by using lentivirus-mediated shRNAs (Supplementary Figure 3A), and performed tumorsphere formation assay. Similar to EZH2 deficiency [18], the experimental results showed that silencing either CDK2 or EZH2 dramatically reduced the primary and secondary tumorsphere formation *in vitro*, suggesting that both CDK2 and its phosphorylation target EZH2 are required for maintenance and self-renewal of BTICs (**Figure 3A**).

To address whether the effect of CDK2 on BTIC population is through phosphorylating EZH2 at T416, we chose a luminal breast cancer cell line T47D, which expresses low levels of EZH2 and contains a small population of BTICs, to generate stable cell lines expressing EZH2^{WT}, EZH2^{T416A}, and EZH2^{T416D} (Supplementary Figure 3B). Then, we performed Hoechest 33342 side population analysis to determine BTICs population in each stable cell line. Compared to vector control cells, those expressing EZH2^{WT} protein had a 3-fold increase in side population, which represents BTIC population (**Figure 3B**). The cells expressing the phospho-mimic EZH2^{T416D} had 7-fold increase in side population (**Figure 3B**). In contrast, a significant reduction in side population was observed in those expressing the phospho-deficient EZH2^{T416A} compared with control cells (**Figure 3B**). Together, these results suggest that T416 phosphorylation of EZH2 by cyclin E/CDK2 is one of the requirements for expansion and maintenance of BTIC population.

To further validate the requirement of EZH2 T416 phosphorylation by CDK2 for expansion

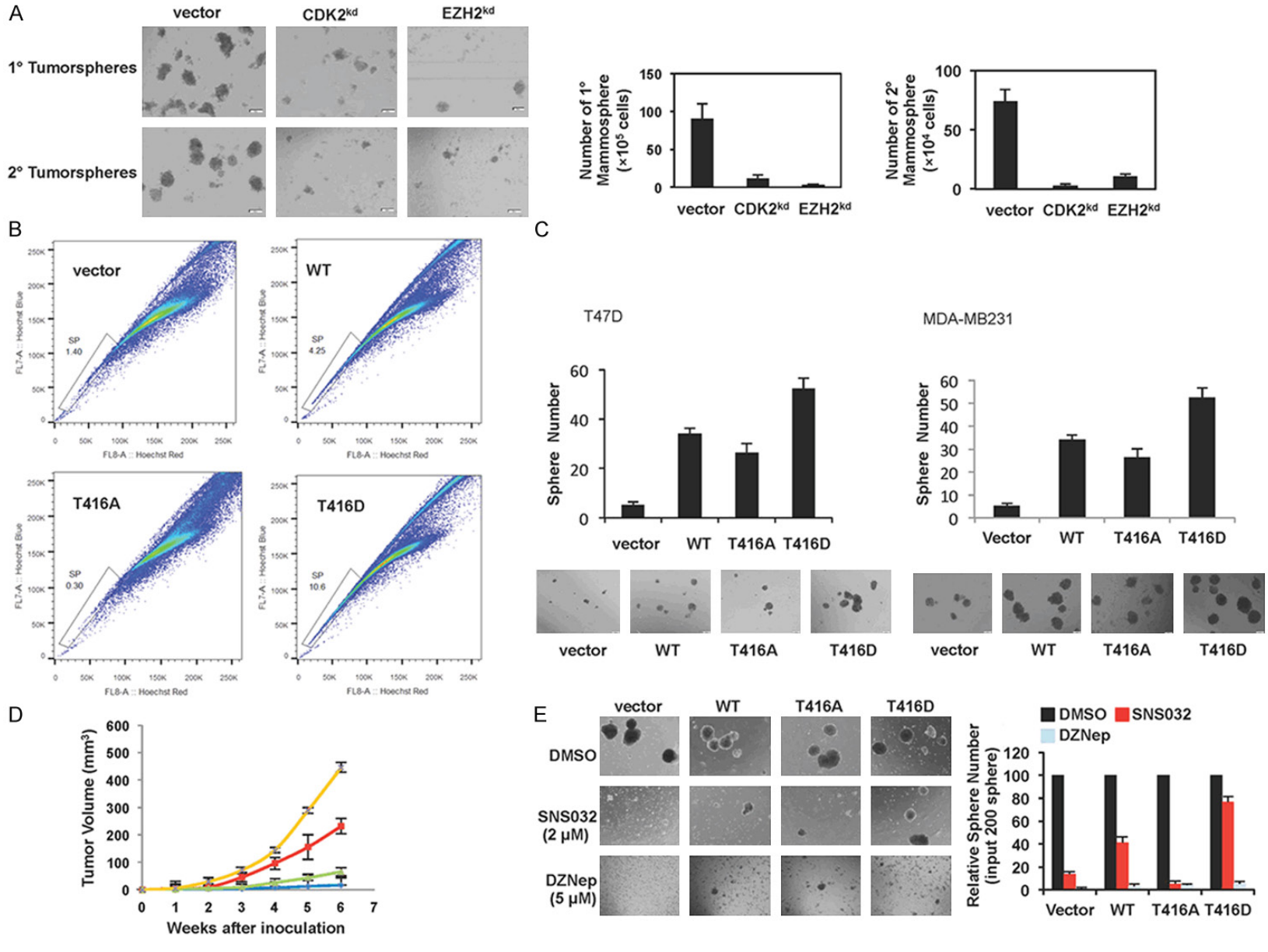
A
vector
CDK2kd
EZH2kd
1° Tumorspheres
2° Tumorspheres
Number of 1° Mammosphere (×10⁵ cells)
Number of 2° Mammosphere (×10⁴ cells)
vector CDK2kd EZH2kd
B
vector
WT
T416A
T416D
SP 1.40
SP 4.25
SP 0.30
SP 10.6
FL7-A :: Hoechst Blue
FL8-A :: Hoechst Red
C
T47D
MDA-MB231
Sphere Number
vector WT T416A T416D
Vector WT T416A T416D
D
Tumor Volume (mm³)
Weeks after inoculation
E
DMSO
SNS032 (2 μM)
DZNep (5 μM)
DMSO SNS032
DZNep
Relative Sphere Number (input 200 sphere)
Vector WT T416A T416D

Figure 3. EZH2 T416 phosphorylation enhances tumorsphere formation and xenograft tumor growth. A. Primary and secondary tumorsphere formation assay for MDA-MB-231 cells with shLuc (control), shCDK2, or shEZH2. Representative images of tumorspheres from the CDK2 and EZH2 knockdown cells are shown. B. Side population analysis was performed with Hoechest 33342 in T47D cells stably expressing control vector, $EZH2^{WT}$, $EZH2^{T416A}$, or $EZH2T^{416D}$. C. Tumorsphere formation assay for T47D and MDA-MB231 cells stable expressing $EZH2^{WT}$, $EZH2T^{416A}$, or $EZH2^{T416D}$. D. Orthotopic xenograft tumor growth of MDA-MB-231 cells expressing control vector, $EZH2^{WT}$, $EZH2T^{416A}$, or $EZH2^{T416D}$. E. Tumorsphere inhibition by a CDK2 or EZH2 inhibitor. Two hundreds of the pre-formed tumorspheres derived from the T47D stable cell lines were treated with CDK2 inhibitor SNS032 (2 μM) or EZH2 inhibitor DZNep (5 μM) for 7 days. Error bars represent ± SEM of two independent experiments.

and maintenance of BTICs, we performed tumorsphere formation assay using the T47D and MDA-MB231 EZH2 stable cell lines established by using lentivirus-mediated gene transfer described in **Figure 2A**. We found that the number of tumorspheres formed by $EZH2^{T416A}$-expressing cells was less than that by $EZH2^{WT}$-expressing cells (**Figure 3C**). In contrast, the $EZH2^{T416D}$-expressing cells had more than 10-fold and 2-fold tumorspheres number in T47D and MDA-MB231-derived cell lines, respectively, compared to vector control (**Figure 3C**). In addition, we also evaluated the effects of EZH2 T416 phosphorylation on a tumor-forming potential in a breast cancer xenograft tumor model. $EZH2^{WT}$-, $EZH2^{T416A}$- or $EZH2^{T416D}$-expressing stable MDA-MB-231 cells (**Figure 2A**) were injected into the mammary fat pad of nude mice, and the tumor size was measured every three days to monitor tumor growth. Consistent with the *in vitro* data, $EZH2^{T416D}$ tumor burdens were significantly larger than that of $EZH2^{WT}$ while those of the $EZH2^{T416A}$ tumors were significantly smaller at 5^{th}- and 6^{th}-week post inoculation (**Figure 3D**). Collectively, these data suggest that cyclin E/CDK2-mediated phosphorylation of EZH2 is critical for the EZH2 function in maintaining BTICs and promoting tumor growth.

EZH2 T416 phosphorylation confers tumorsphere resistance to a CDK2 inhibitor

Hyperactivation of CDKs, such as CDK2, has been shown to favor tumor development via expansion of cancer stem or progenitor cells through unscheduled cell division in either of these upper lineage breast cancer cell populations [30, 31]. Therefore, inhibition of CDK2 may be a suitable intervention and druggable strategy for treating TNBC. Our above findings showed that EZH2 T416 phosphorylation can enhance tumorsphere growth. Therefore, we developed a tumorsphere killing assay using TNBC-derived spheres as tissue culture test spheres. To assess the CDK2- and EZH2-dependency on tumorsphere maintenance, tumorspheres of T47D stable cell lines used in **Figure 3B** were established. Since each cell line has different capacity for primary tumorsphere formation (**Figure 3C**), the pre-formed sphere number (Ø > 100 μm) was adjusted to 200-spheres per well before adding chemical inhibitors for CDK2 and EZH2. $EZH2^{WT}$ stable cells treated with CDK2-specific inhibitor SNS032 had a 60% reduction in sphere number after drug treatment for 7 days compared with untreated cells (**Figure 3E**). The number of spheres expressing phospho-mimic $EZH2^{T416D}$ was reduced by about 20%, exhibiting significant resistance to SNS032 treatment (**Figure 3E**). Because $EZH2^{WT}$ is CDK2-dependent but both $EZH2^{T416A}$ and $EZH2^{T416D}$ are CDK2-independent, it is possible that 20% reduction of $EZH2^{T416D}$ tumorspheres is due to endogenous EZH2. In contrast, the pre-formed tumorspheres derived from all stable cell lines were sensitive to EZH2 inhibitor DZNep (**Figure 3E**), suggesting that CDK2 is the upstream regulator of EZH2. Moreover, expression of T416 phosphorylated EZH2-mimicking form, $EZH2^{T416D}$, efficiently rescued tumorsphere survival in the presence of the CDK2 inhibitor. Taken together, EZH2 T416 phosphorylation by CDK2 plays a critical role in expansion and maintenance of BTICs, in particular of BLBC/TNBC.

EZH2 T416 phosphorylation in human TNBC tissue specimens

To investigate the clinical significance of EZH2 T416 phosphorylation, we used our pT416 EZH2 monoclonal antibody for IHC staining of a cohort of 122 primary TNBC tissues. Examination of the TNBC cohort demonstrated that when pT416-EZH2 was elevated, there was a decreasing trend for patient survival with statistical significance (P = 0.049; **Figure 4A** and **4B**). These data suggest that pT416-EZH2 could serve as a prognostic biomarker to predict TNBC survival. In addition, pT416-EZH2 may be

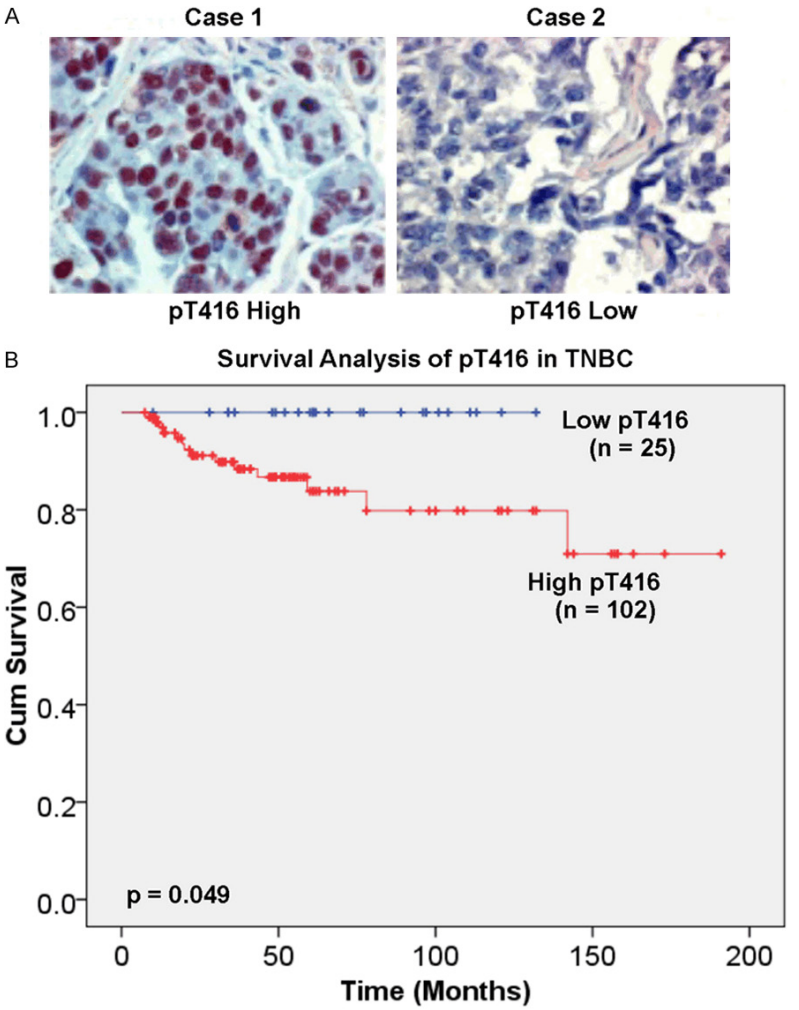

Figure 4. Correlation between pT416 EZH2 level and survival in triple-negative breast cancer patients. A. Representative case of high EZH2-T416 phosphorylation (pT416; n = 102) and low EZH2-T416 (n = 25) phosphorylation are shown. B. Survival analysis of patients with high and low pT416 in TNBC patients. Log rank P = 0.049.

directly linked to cyclin E expression and CDK2 activity. Indeed, EZH2 expression was correlated to cyclin E expression only in TNBC but not non-TNBC (**Tables 1** and **2**). EZH2 T416 phosphorylation, which is primarily induced by cyclin E/CDK2 in TNBC, is clinically significant, suggesting a rationale for the development of a CDK2 inhibitor-based therapy for TNBC patients positive for pT416-EZH2.

Discussion

Our findings in TNBC cell lines and human breast cancer tissues support the hypothesis that phosphorylation of EZH2 T416 by CDK2 is able to promote tumorigenesis and cell invasion in TNBC. Analysis of the TCGA database showed that EZH2 is highly expressed in TNBC and HER2-enriched breast cancer (Supplementary Figure 4). Our IHC staining data from human primary TNBCs uncovered that elevated EZH2 was closely correlated with cyclin E, and EZH2 and cyclin E were co-expressed with clinical significance in TNBC patients compared to non-TNBCs. Moreover, human primary tumor tissues staining with specific antibodies against pT416-EZH2 revealed that increased pT416-EZH2 level in TNBC is negatively correlated to patient survival. These findings suggest that there is a tight link between cyclin E/CDK2 and EZH2 expression in this specific subtype of breast cancer.

Currently, there are limited targeted therapies available to treat TNBC. In addition to discovering new drug targets for TNBC, it is also critical to identify new biomarkers that can predict the onset and progression of TNBC tumors as well as therapeutic resistance. Here, we demonstrated that cyclin E/CDK2 phosphorylates EZH2 at T416 in breast cancer cells *in vivo*. Phosphorylation of EZH2 T416 by CDK2 is required for expansion and maintenance of BTICs *in vitro*. Therefore, EZH2 phosphorylation at T416 may play a critical role in tumorigenesis and tumor progression of BLBC/TNBC and may be a potential biomarker for BLBC/TNBC. In addition, our findings also showed that both CDK2 and EZH2 inhibitors can directly or indirectly block EZH2 function in breast cancer cells, leading to inhibition of BTIC survival. On the basis of these results, administration of CDK2 and EZH2 inhibitors may have therapeutic potential to BLBC/TNBC patients. Currently, clinical trials of both CDK2 and EZH2

inhibitors are ongoing. The components of this study describe a rationale to proceed to preclinical animal models with the perspective of later clinical studies for designing new therapeutic regimens of CDK inhibitors and epigenetically-targeted inhibitors for the treatment of BLBC/TNBC patients.

Acknowledgements

This study was funded in part by the following: Susan G. Komen Foundation (SAC110016); Ministry of Science and Technology, International Research-intensive Centers of Excellence in Taiwan (I-RiCE; MOST 104-2911-I-002-302); Ministry of Health and Welfare, China Medical University Hospital Cancer Research Center of Excellence (MOHW104-TDU-B-212-124-002); and Center for Biological Pathways.

Disclosure of conflict of interest

None.

Address correspondence to: Mien-Chie Hung, Department of Molecular and Cellular Oncology, The University of Texas MD Anderson Cancer Center, Unit 108, Houston, Texas 77030. E-mail: mhung@mdanderson.org

References

[1] Perou CM, Sorlie T, Eisen MB, van de Rijn M, Jeffrey SS, Rees CA, Pollack JR, Ross DT, Johnsen H, Akslen LA, Fluge O, Pergamenschikov A, Williams C, Zhu SX, Lonning PE, Borresen-Dale AL, Brown PO and Botstein D. Molecular portraits of human breast tumours. Nature 2000; 406: 747-752.

[2] Sorlie T, Perou CM, Tibshirani R, Aas T, Geisler S, Johnsen H, Hastie T, Eisen MB, van de Rijn M, Jeffrey SS, Thorsen T, Quist H, Matese JC, Brown PO, Botstein D, Lonning PE and Borresen-Dale AL. Gene expression patterns of breast carcinomas distinguish tumor subclasses with clinical implications. Proc Natl Acad Sci U S A 2001; 98: 10869-10874.

[3] Dent R, Trudeau M, Pritchard KI, Hanna WM, Kahn HK, Sawka CA, Lickley LA, Rawlinson E, Sun P and Narod SA. Triple-negative breast cancer: clinical features and patterns of recurrence. Clin Cancer Res 2007; 13: 4429-4434.

[4] Reis-Filho JS and Tutt AN. Triple negative tumours: a critical review. Histopathology 2008; 52: 108-118.

[5] Lehmann BD, Bauer JA, Chen X, Sanders ME, Chakravarthy AB, Shyr Y and Pietenpol JA. Identification of human triple-negative breast cancer subtypes and preclinical models for selection of targeted therapies. J Clin Invest 2011; 121: 2750-2767.

[6] Bertucci F, Finetti P, Cervera N, Esterni B, Hermitte F, Viens P and Birnbaum D. How basal are triple-negative breast cancers? Int J Cancer 2008; 123: 236-240.

[7] de Ronde JJ, Hannemann J, Halfwerk H, Mulder L, Straver ME, Vrancken Peeters MJ, Wesseling J, van de Vijver M, Wessels LF and Rodenhuis S. Concordance of clinical and molecular breast cancer subtyping in the context of preoperative chemotherapy response. Breast Cancer Res Treat 2010; 119: 119-126.

[8] Rakha EA and Ellis IO. Triple-negative/basal-like breast cancer: review. Pathology 2009; 41: 40-47.

[9] Rakha EA, Reis-Filho JS and Ellis IO. Basal-like breast cancer: a critical review. J Clin Oncol 2008; 26: 2568-2581.

[10] Sorlie T. Molecular portraits of breast cancer: tumour subtypes as distinct disease entities. Eur J Cancer 2004; 40: 2667-2675.

[11] Liedtke C, Mazouni C, Hess KR, Andre F, Tordai A, Mejia JA, Symmans WF, Gonzalez-Angulo AM, Hennessy B, Green M, Cristofanilli M, Hortobagyi GN and Pusztai L. Response to neoadjuvant therapy and long-term survival in patients with triple-negative breast cancer. J Clin Oncol 2008; 26: 1275-1281.

[12] Badve S, Dabbs DJ, Schnitt SJ, Baehner FL, Decker T, Eusebi V, Fox SB, Ichihara S, Jacquemier J, Lakhani SR, Palacios J, Rakha EA, Richardson AL, Schmitt FC, Tan PH, Tse GM, Weigelt B, Ellis IO and Reis-Filho JS. Basal-like and triple-negative breast cancers: a critical review with an emphasis on the implications for pathologists and oncologists. Mod Pathol 2011; 24: 157-167.

[13] Shastry M and Yardley DA. Updates in the treatment of basal/triple-negative breast cancer. Curr Opin Obstet Gynecol 2013; 25: 40-48.

[14] Simon JA and Kingston RE. Mechanisms of polycomb gene silencing: knowns and unknowns. Nat Rev Mol Cell Biol 2009; 10: 697-708.

[15] Di Croce L and Helin K. Transcriptional regulation by Polycomb group proteins. Nat Struct Mol Biol 2013; 20: 1147-1155.

[16] De Brot M, Rocha RM, Soares FA and Gobbi H. Prognostic impact of the cancer stem cell related markers ALDH1 and EZH2 in triple negative and basal-like breast cancers. Pathology 2012; 44: 303-312.

[17] Hussein YR, Sood AK, Bandyopadhyay S, Albashiti B, Semaan A, Nahleh Z, Roh J, Han HD, Lopez-Berestein G and Ali-Fehmi R. Clinical

and biological relevance of enhancer of zeste homolog 2 in triple-negative breast cancer. Hum Pathol 2012; 43: 1638-1644.
[18] Chang CJ, Yang JY, Xia W, Chen CT, Xie X, Chao CH, Woodward WA, Hsu JM, Hortobagyi GN and Hung MC. EZH2 promotes expansion of breast tumor initiating cells through activation of RAF1-beta-catenin signaling. Cancer Cell 2011; 19: 86-100.
[19] Gonzalez ME, Moore HM, Li X, Toy KA, Huang W, Sabel MS, Kidwell KM and Kleer CG. EZH2 expands breast stem cells through activation of NOTCH1 signaling. Proc Natl Acad Sci U S A 2014; 111: 3098-3103.
[20] Voduc D, Nielsen TO, Cheang MC and Foulkes WD. The combination of high cyclin E and Skp2 expression in breast cancer is associated with a poor prognosis and the basal phenotype. Hum Pathol 2008; 39: 1431-1437.
[21] Kaneko S, Li G, Son J, Xu CF, Margueron R, Neubert TA and Reinberg D. Phosphorylation of the PRC2 component Ezh2 is cell cycle-regulated and up-regulates its binding to ncRNA. Genes Dev 2010; 24: 2615-2620.
[22] Chen S, Bohrer LR, Rai AN, Pan Y, Gan L, Zhou X, Bagchi A, Simon JA and Huang H. Cyclin-dependent kinases regulate epigenetic gene silencing through phosphorylation of EZH2. Nat Cell Biol 2010; 12: 1108-1114.
[23] Wei Y, Chen YH, Li LY, Lang J, Yeh SP, Shi B, Yang CC, Yang JY, Lin CY, Lai CC and Hung MC. CDK1-dependent phosphorylation of EZH2 suppresses methylation of H3K27 and promotes osteogenic differentiation of human mesenchymal stem cells. Nat Cell Biol 2011; 13: 87-94.
[24] Wu SC and Zhang Y. Cyclin-dependent kinase 1 (CDK1)-mediated phosphorylation of enhancer of zeste 2 (Ezh2) regulates its stability. J Biol Chem 2011; 286: 28511-28519.
[25] Minnebo N, Gornemann J, O'Connell N, Van Dessel N, Derua R, Vermunt MW, Page R, Beullens M, Peti W, Van Eynde A and Bollen M. NIPP1 maintains EZH2 phosphorylation and promoter occupancy at proliferation-related target genes. Nucleic Acids Res 2013; 41: 842-854.
[26] Lien HC, Hsiao YH, Lin YS, Yao YT, Juan HF, Kuo WH, Hung MC, Chang KJ and Hsieh FJ. Molecular signatures of metaplastic carcinoma of the breast by large-scale transcriptional profiling: identification of genes potentially related to epithelial-mesenchymal transition. Oncogene 2007; 26: 7859-7871.
[27] van den Heuvel S and Harlow E. Distinct roles for cyclin-dependent kinases in cell cycle control. Science 1993; 262: 2050-2054.
[28] Sasaki T, Maier B, Koclega KD, Chruszcz M, Gluba W, Stukenberg PT, Minor W and Scrable H. Phosphorylation regulates SIRT1 function. PLoS One 2008; 3: e4020.
[29] Bracken AP, Pasini D, Capra M, Prosperini E, Colli E and Helin K. EZH2 is downstream of the pRB-E2F pathway, essential for proliferation and amplified in cancer. EMBO J 2003; 22: 5323-5335.
[30] Corsino PE, Davis BJ, Norgaard PH, Parker NN, Law M, Dunn W and Law BK. Mammary tumors initiated by constitutive Cdk2 activation contain an invasive basal-like component. Neoplasia 2008; 10: 1240-1252.
[31] Duong MT, Akli S, Macalou S, Biernacka A, Debeb BG, Yi M, Hunt KK and Keyomarsi K. Hbo1 is a cyclin E/CDK2 substrate that enriches breast cancer stem-like cells. Cancer Res 2013; 73: 5556-5568.

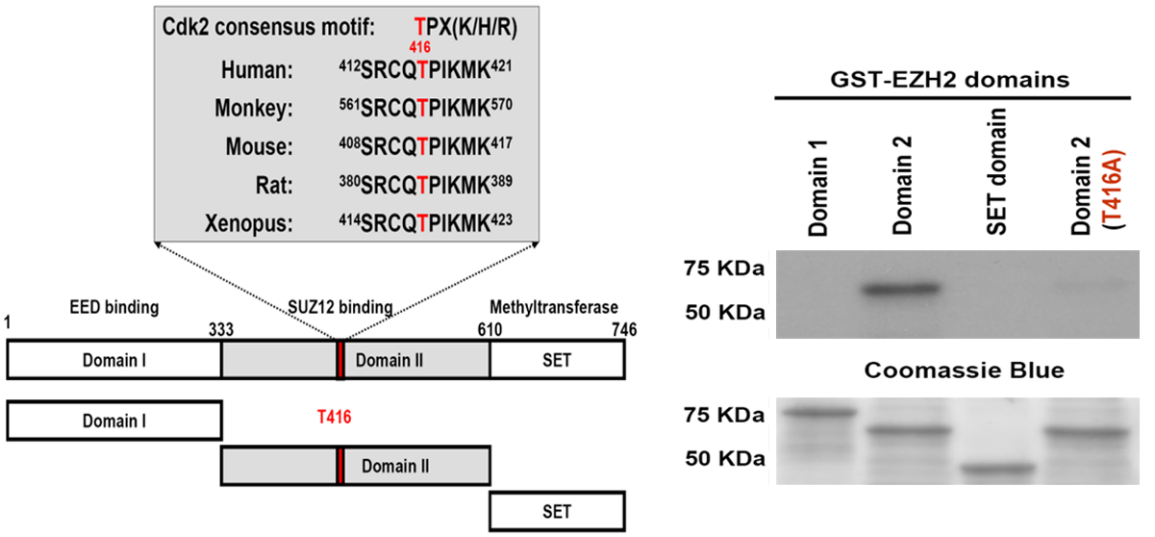

Supplementary Figure 1. Left, *in silico* analysis of the EZH2 T416. T416 was mapped to an evolutionary conserved CDK2 consensus motif (K(R)S(T)PXK(R), where X is any residue. Right, *in vitro* kinase assays were conducted by incubating GST-EZH2 (1-333), GST-EZH2 (334-610), GST-EZH2 (611-746), or T416A mutant GST-EZH2 (334-610) with recombinant active Cyclin E/CDK2 complex. Samples were resolved using autoradiography.

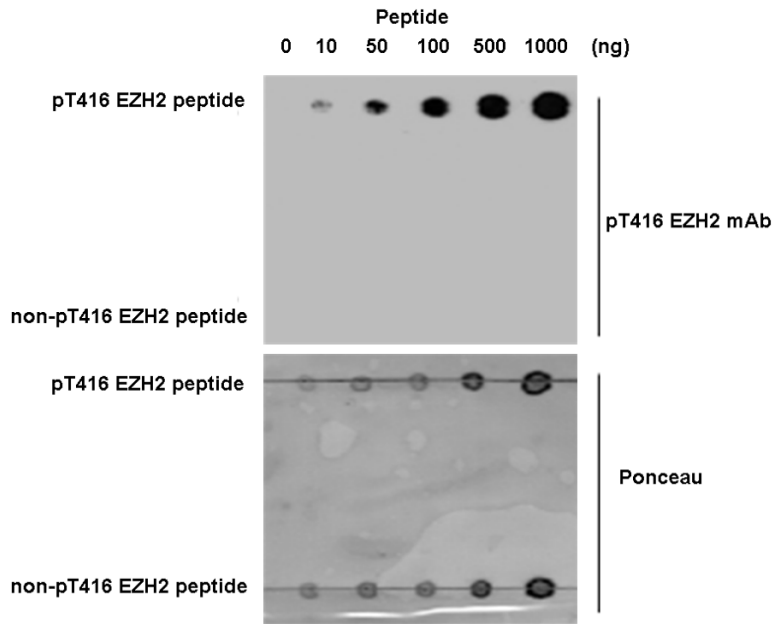

Supplementary Figure 2. Dot blot characterization of phospho-T416 EZH2 antibody under phospho-peptide competition assay. Phospho- or non-phospho-peptides were immunoblotted with a phospho-T416-EZH2 antibody.

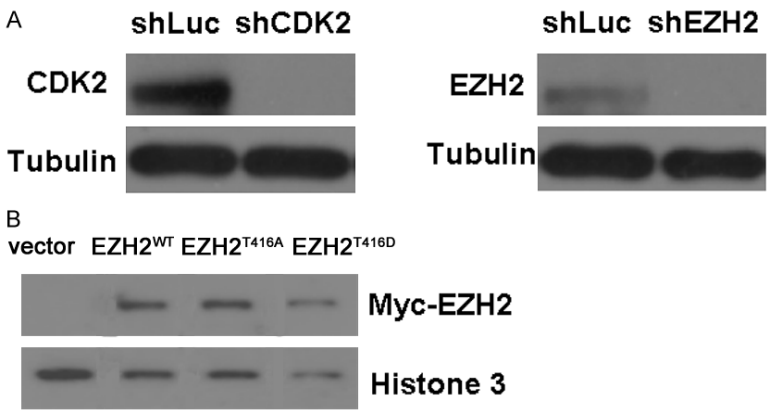

Supplementary Figure 3. A. Western blot analysis of CDK2 and EZH2 expression in CDK2 and EZH2 knockdown MDA-MB-231 cells. B. Expression of myc-tagged $EZH2^{WT}$, $EZH2^{T416A}$, $EZH2^{T416D}$ in T47D cells was determined by Western blot analysis with anti-myc antibody. Histone 3 was used as a loading control.

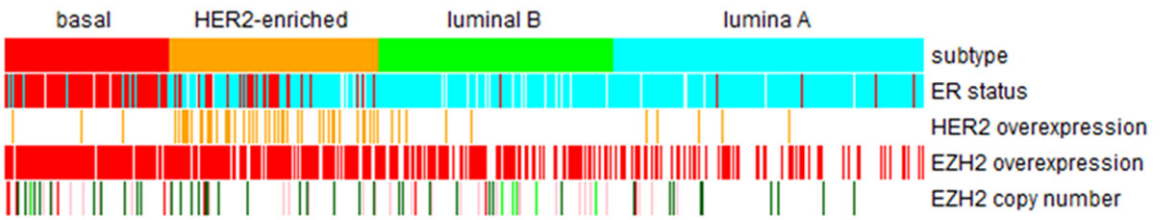

Supplementary Figure 4. Heat map of EZH2 expression levels in different subtypes of breast cancers (TCGA database).